

## The Effect of Boron Content, Crystal Structure, Crystal Size on the Hardness and the Corrosion Resistance of Electrodeposited Ni-B Coatings

J.R. López<sup>1,2</sup>, P.F. Méndez<sup>1,2</sup>, J. J. Pérez-Bueno<sup>1</sup>, G. Trejo<sup>1</sup>, G. Stremmsdoerfer<sup>3</sup>, Y. Meas<sup>1,\*</sup>

<sup>1</sup> Centro de Investigación y Desarrollo Tecnológico en Electroquímica (CIDETEQ), Parque Tecnológico Querétaro, Sanfandila, Pedro Escobedo, Querétaro, P.O. Box. 76700, México

<sup>2</sup> Universidad Autónoma de Sinaloa, Facultad de Ciencias Químico Biológicas, Ciudad Universitaria, Culiacán Sinaloa, CP 80000, México

<sup>3</sup>EcoleCentrale of Lyon, Tribological& Dynamical Systems Laboratory, 36 Avenue Guy de Collongue, P.O. Box 163, 69134 Ecully, France

\*E-mail: [yunnymeas@cideteq.mx](mailto:yunnymeas@cideteq.mx)

Received: 9 November 2015 / Accepted: 3 December 2015 / Published: 4 May 2016

---

In this work Ni–B coatings with different boron content (0.6 to approximately 3.4 wt.%) were produced by electrodeposition from a sulfamate bath containing dimethylamineborane (DMAB). The influence of boron concentration on the structure, morphology, crystal size and hardness of the coatings was investigated using plasma emission spectroscopy (ICP), scanning electron microscopy (SEM) and X-ray diffractometry (XRD). Crystal size and structure were evaluated in both as-plated and thermal-treatment conditions to establish their relationship to the hardness of the coating. The corrosion resistance of the coatings was evaluated in 5% NaCl, employing electrochemical polarization measurement and salt spray testing. The results showed that the increased hardness of the as-plated Ni-B coatings is primarily caused by a reduction in crystal size rather than boron composition. Thus, Ni-B coatings can be produced with high hardness ( $716 \pm 22.5$  HV) with a relatively low boron composition (1.8 wt. %). On the other hand, Ni-B coatings produced after thermal treatment showed that hardness depends on two factors: composition ( $\text{Ni}_3\text{B}$ ) and crystal size, achieving the highest hardness at 350°C ( $1105 \pm 19.4$  HV). Unless the obtained Ni-B coatings showed a high hardness, the corrosion resistance is low due to the presence of cracks.

---

**Keywords:** Ni-B, electroplating, hardness, corrosion, sulfamate bath

### 1. INTRODUCTION

Ni-B coatings produced by both electroless and electroplating techniques are important to industry, because coatings with high hardness and good wear resistance can be produced by these

relatively simple processes; compared to other techniques such as physical vapor deposit (PVD) and chemical vapor deposition (CVD) [1, 2]. These coatings can reach hardness up to 1200 HV, after thermal treatment [3-5], with a wear resistance (tribological properties) that may be similar to or greater than chromium coatings [3, 6, 7].

Ni-B coatings are produced with the electroless technique, employing electrolytic baths containing nickel salts and reducing agents such as sodium borohydride [6, 8-10] or dimethylamineborane (DMAB) [11-14]. In addition to these components, these baths must also include complexing agents and stabilizers to reduce their spontaneous decomposition [2, 15]. As a result, electroless baths have complex compositions that are difficult to control and have limited lifespans [16, 17]. Electroplating, an alternative to electroless plating, is easier to control because it employs an electrolytic bath that requires lower maintenance than the electroless process.

Recently, Ni-B coatings have been produced by electroplating from electrolytic baths containing dimethylamineborane (DMAB) [5, 18,19], triethylamineborane (TMAB) [4,5,20] or sodium decahydrodecaborate ( $\text{Na}_2\text{B}_{10}\text{H}_{10}$ ) [7] that have mechanical properties similar to or better than Ni-B coatings produced by electroless. Most research has used Watts baths, and electrolytic baths that contain sulfamate salts have rarely been studied. However, these sulfamates electrolytic baths have important advantages, such as simple composition, the ability to operate at high current densities, low internal stress, and they produce coatings with good ductility [21].

In this work, nickel coatings were produced using a sulfamate bath with different concentrations of DMAB, with the objective of evaluating the effect of composition, microstructure and crystal size on the hardness of the coating. Microstructure and crystal size were measured before and after thermal treatment in order to establish their relationship to the increase in the hardness of the coatings.

## 2. MATERIALS AND METHODS

In this study, Ni-B electroplating was done using an electrolytic bath based on sulfamate. Composition and operating conditions are presented in Table 1. Boron (B) was incorporated in the Ni coatings by adding dimethylamineborane (DMAB) to the electrolytic bath. The use of DMAB to produce Ni-B coating by electroless is reported in the literature [11-14], and recently it has been used as a boron source to produce Ni-B coatings by electroplating [5, 18, 19].

Ni-B electrodeposits with a thickness of about 20  $\mu\text{m}$  were produced using a parallel-plate cell with a volume of 500 mL, a nickel anode (high purity) and steel plates as cathodes (AISI 1006: 0.074% C, 0.004% S, 0.008% P, 0.245% Si, 0.174% Mn, size: 65 x 70 x 1 mm). Prior to electroplating, the steel plates were immersed in an alkaline solution at 80 °C for 10 min and then etched in a sulfamic acid solution (30 g/L) for 15 s.

**Table 1.** Composition and operating conditions of the electrolytic bath used to produce Ni-B coatings

<b>Composition</b>	Nickel sulfamate	400 g/L
	Boric acid	30 g/L
	Commercial surfactant (AA)	3 - 6 mL/L
	Dimethylamine borane (DMAB)	1, 3 y 5 g/L
<b>Operating conditions</b>	pH	3.0 - 3.5
	Temperature	45 °C
	Current density	30 mA/cm <sup>2</sup>
	Mechanical agitation	350 rpm
	Time	37 min

The composition of the coatings was determined by plasma emission spectroscopy (ICP). The analyzed coatings were formed on a stainless steel substrate to facilitate their removal and dissolution in nitric acid.

The hardness of the coatings was measured with a Vickers diamond indenter, applying a load of 200 gf. For each sample, 10 measurements were performed to obtain an average value.

The morphology of the coatings was determined by scanning electron microscopy (SEM) using a JEOL- 5400LV microscope. The texture and grain size of the Ni-B coatings were determined by X-Ray diffraction (XRD) using a Bruker AXS D8 Advance diffractometer.

The polarization curves were carried out in a three-electrodes glass cell. A calomel (SCE) and platinum mesh were used as reference and counter electrode respectively. A PAR 263A potentiostat-galvanostat was used to carry out the electrochemical experiments. Measurements were done in an electrolytic solution consisted of NaCl 5% at 25 °C with a scan rate of 0.17 mV/s according the standard ASTM G5 [22]. All the experiments were carried out after 2 hr to stabilize the equilibrium potential in the electrolytic solution. Finally, exposure test were done in a Q-FOG CCT-600 salt spray corrosion test chamber according ASTM B117 standard [23] and ISO 10289 norm [24]. The criterion for determining the failure of the coating was the presence of the first point of red corrosion.

### 3. RESULTS AND DISCUSSION

#### 3.1 Effect of the concentration of DMAB in the electrolytic bath on the properties of the coatings

##### 3.1.1 Effect of the boron composition on the hardness of Ni-B coatings

Composition and hardness of the nickel coatings were tested as a function of the concentration of DMAB in the electrolytic bath. The electroplating speed of Ni-B coating was approximately 36  $\mu\text{m/h}$  at a current density of 30 mA/cm<sup>2</sup>.

The boron composition in the Ni-B coatings is shown in Table 2. It can be observed that boron content in the Ni coatings increases with the concentration of DMAB in the bath, co-deposition of B in the coatings is enhanced by DMAB concentration in the electrolytic bath.

**Table 2.** Composition of Ni- B coatings produced by electrodeposition

DMAB Concentration	Boron Composition
1 g/L	0.59 %
3 g/L	1.85 %
5 g/L	3.40 %

The mechanism of incorporating boron into Ni-B coating produced by electrodeposition is not clearly understood. However, one possibility is that DMAB is adsorbed and later decomposed forming elemental boron on the surface (catalytic) of Ni previously formed. This is similar to an autocatalytic process (electroless) with the difference that the activation energy or propagation of this reaction is controlled by electric power and not by thermal energy. In this manner, boron incorporation in the coating should be related to the Ni reduction rate and the adsorption and decomposition of DMAB rate on the cathode, as suggested by Krishnaveni *et al.* [18].

If the Ni reduction rate is kept constant by controlling the operating conditions of the bath (agitation, *j*, T and pH), then B incorporation is given by the DMAB decomposition rate, which is a function of its concentration in the electrolytic bath. It is important to highlight that, for an electrolytic bath with DMAB concentration of 5 g/L, deposition on the walls of the electrolytic cell was observed, which indicates that under these conditions Ni-B deposition resulted from the electroless process. This phenomenon was also observed by Ogihara *et al.* [5] during Ni-B electrodeposition with DMAB at concentrations greater than 3 g/L. In this work, at 1 and 3 g/L of DMAB, the electroless process was not significant. This was proven by introducing a steel plate in the electrolytic bath, after one hour of immersion without applying current, it was possible to verify that there was no coating on the substrate (based on weight differences).

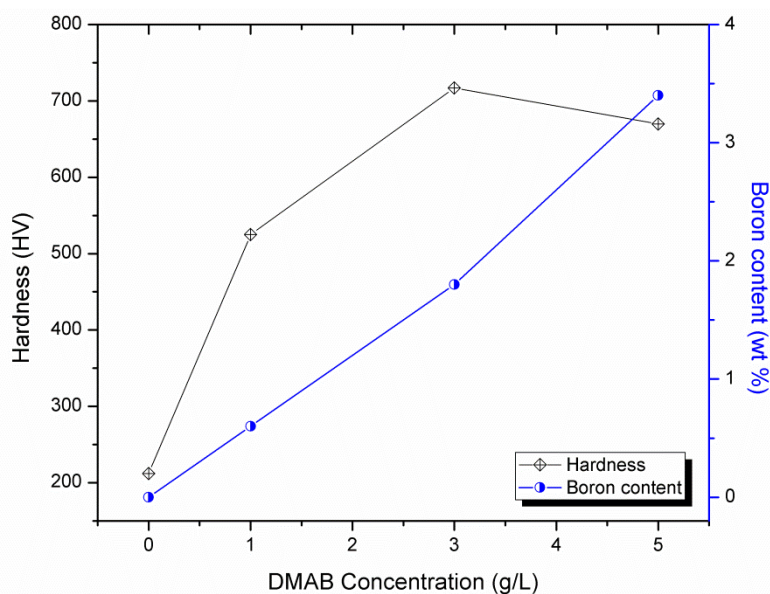


**Figure 1.** Hardness and boron composition for Ni-B coatings produced from an electrolytic bath with different DMAB concentrations.

Figure 1 shows the hardness values and boron composition of Ni-B coatings produced from an electrolytic bath at various DMAB concentrations. In this figure, it can be seen that the hardness of the coatings increases with DMAB concentration until 3 g/L. At this concentration, a coating was produced with the highest level of hardness:  $716 \pm 22.5$  HV. At a higher DMAB concentration (5 g/L), in contrast to the boron composition in the coating, the hardness decreased slightly to  $(669 \pm 25.6)$  HV. However, considering the standard deviation values in these measurements, in this concentration range, hardness is practically constant. These results indicate that hardness of Ni coatings produced from an electrolytic bath with DMAB is not only clearly related to the B composition in the coating, in this way, studies of crystalline structure and crystal size were done to investigate their influence on Ni coatings hardness.

### 3.1.2 Characterization of Ni- B coatings

Figure 2 shows the X -ray diffraction spectra obtained for Ni coatings with different boron composition. All of the spectra only showed the signal corresponding to metallic Ni; there was no discernible signal corresponding to B or Ni-B alloy.

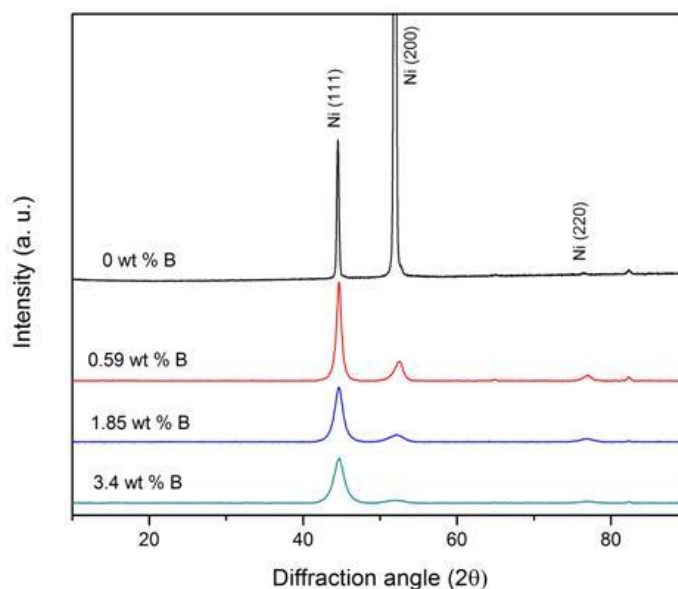


**Figure 2.** XRD spectra for Ni-B coatings with different B content produced from an electrolytic bath with different DMAB concentrations: (a) 0 %, (b) 0.59%, (c) 1.85% and (d) 3.40%.

This suggests that boron atoms are finely deposited in the crystalline lattice (face centered cubic, fcc) of Ni as proposed by Ogihara *et al.* [5]. Ni coatings produced in an absence of DMAB (0 wt %) showed a crystalline structure (fcc) with a preferential growth on the plane (200) followed by the (111) plane. This feature was reported for electrodeposits produced from sulfamate baths [25, 26]. Incorporation of boron in the coating significantly modifies the structure of the coatings. In the spectra,

it can be observed that the diffraction signals for metallic Ni become wider with reduced intensity as the amount of B increases. These properties are attributed to a decrease in crystal size.

Co-deposition of boron in Ni coatings also modifies the texture of the coatings, from a preferential texture (200) to (111). Preferential orientation values, determined by the ratio between peak intensity 111 and 200 ( $I_{(111)} / I_{(200)}$ ) and the crystal size (calculated by the Scherrer equation, considering the preferential peak) are shown in table 3. These values clearly show an increase in the preferred orientation (111) and a significant decrease in crystal size, depending on B composition in the coating. It is evident that the modification in the preferred orientation and decrease in the size of crystals are a result of the inclusion and rearrangement of B atoms in the Ni crystalline lattice (fcc). When 3.4 wt.% of B is incorporated in the coating, the lattice parameter (a) of the crystalline lattice (fcc) decreases from 3.507 Å to 3.490 Å with respect to a free boron coating. This decrease is related to the replacement of Ni atoms, which have an atomic radius of 1.24 Å, by B atoms that have a smaller atomic radius ( $r = 0.97$  Å). Similar behavior was observed by Bekish *et al.* [7] during Ni-B electrodeposition from a Watts-type bath.

**Table 3.** Preferential orientation ( $I_{111}/I_{200}$ ) and crystal size depending on B composition in the coating.

B Composition (wt%)	$I_{(111)} / I_{(200)}$	Crystal Size (nm)
0	0.15	27.3
0.59	5.1	11.6
1.85	7.7	6.9
3.40	15.9	5.5

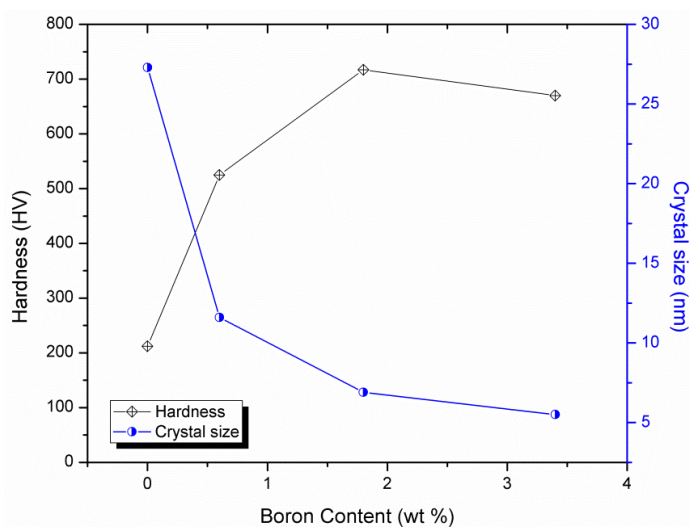


**Figure 3.** Hardness and crystal size as a function of boron content in the Ni-B electrodeposits.

Figure 3 shows the hardness values and crystal size depending on B composition of the coating. From these results, it can be observed that as B composition increases from 1.8 to 3.4 wt.% (there is

not a substantial decrease in crystal size, 1.4 nm). This may be the reason that hardness does not change significantly in this concentration range (as shown in Figure 1). This figure shows that hardness varies inversely with the crystal size of the coatings and that hardness does not only depend on the amount of B co-deposited. This indicates that it is not necessary to incorporate large amounts of boron in the coating to substantially increase hardness.

Figure 4 shows the morphology of the Ni coatings produced from an electrolytic bath with different concentrations of DMAB. Ni coatings produced in the absence of DMAB (Figure 4a) reveals a homogeneous surface with pyramid-shaped grains, which is the typical morphology observed for Ni coatings produced from a sulfamate bath [25, 27].

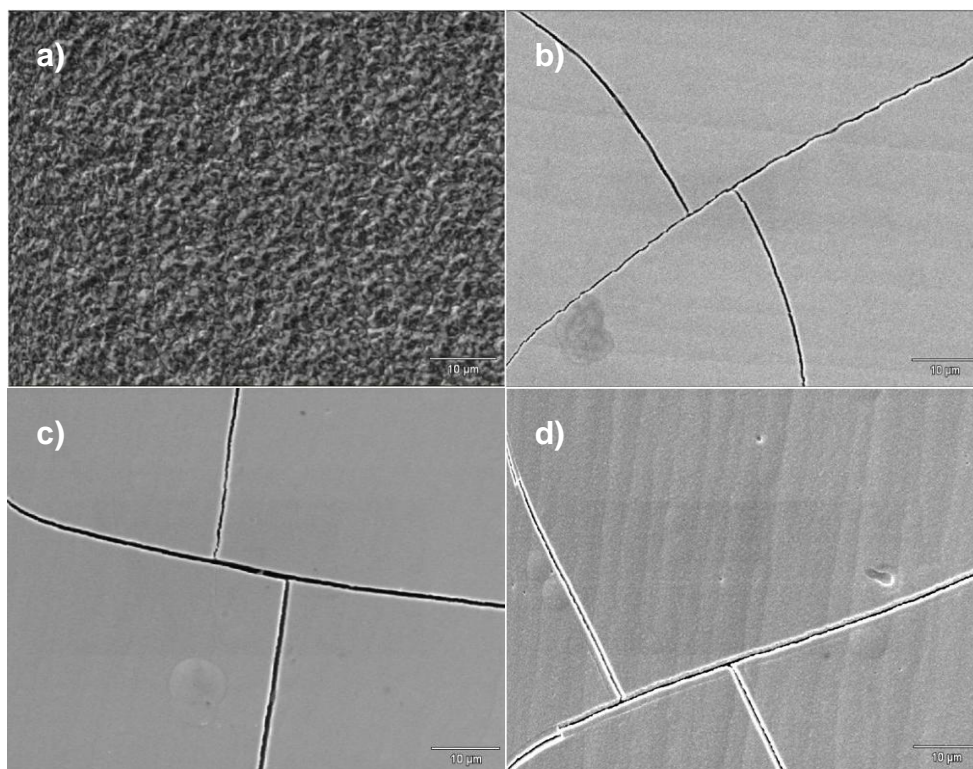


**Figure 4.** SEM image of the surface (2000X) of Ni-B electrodeposits produced from a bath with different DMAB concentration: a) 0 g/L DMAB, b) 1 g/L DMAB, c) 3 g/L DMAB and d) 5 g/L DMAB.

The coatings produced in the presence of DMAB (Fig. 4b, 4c and 4d) show a homogeneous surface with very fine grain size. Unlike Ni coatings produced in the absence of DMAB, these coatings have surface micro-fissures, indicating a very high level of internal stress. Micro-fissures in such coatings were also observed by Krishnaveni *et al.* [18] who suggested that Ni coatings have very high internal stress due to an increase in the hydrogen evolution reaction generated by DMAB decomposition. This result is consistent with the SEM images obtained, which show that the Ni-B coating produced with the highest DMAB concentration (5 g/L) shows pitting generated by hydrogen bubbles.



### 3.2 Effect of thermal treatment on Ni- B coatings

#### 3.2.1 Crystal structure

XRD studies were done to evaluate the structural changes in Ni-B coatings during thermal treatment. Figure 5 shows the XRD spectra obtained for Ni-B coatings containing (B: 1.8 to 3.4 wt.%), before and after thermal treatment (250 to 500 ° C) for 1 h.

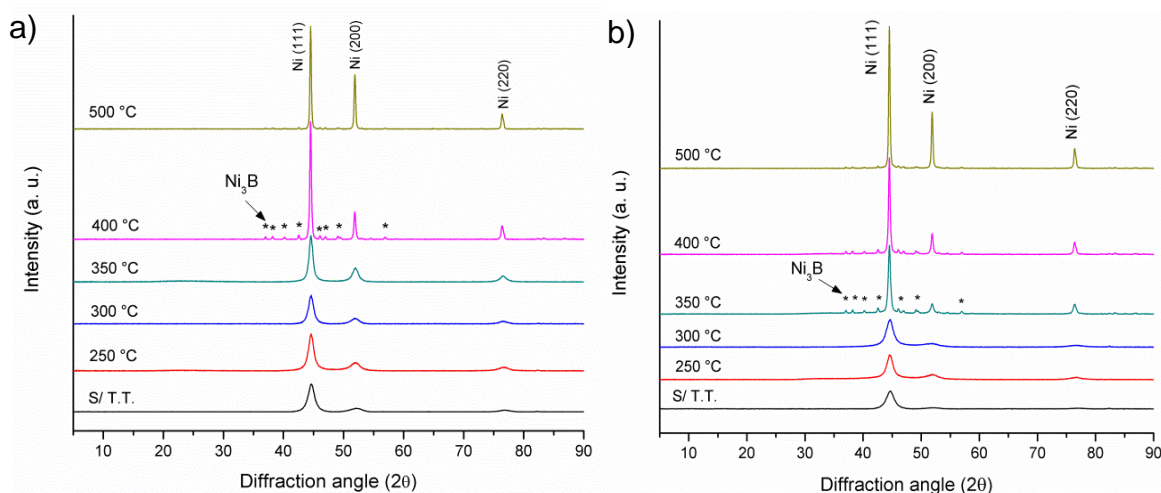


**Figure 5.** XRD spectra of Ni-B coatings with different B composition before and after thermal treatment: a) 1.85 % B and b) 3.40% B.

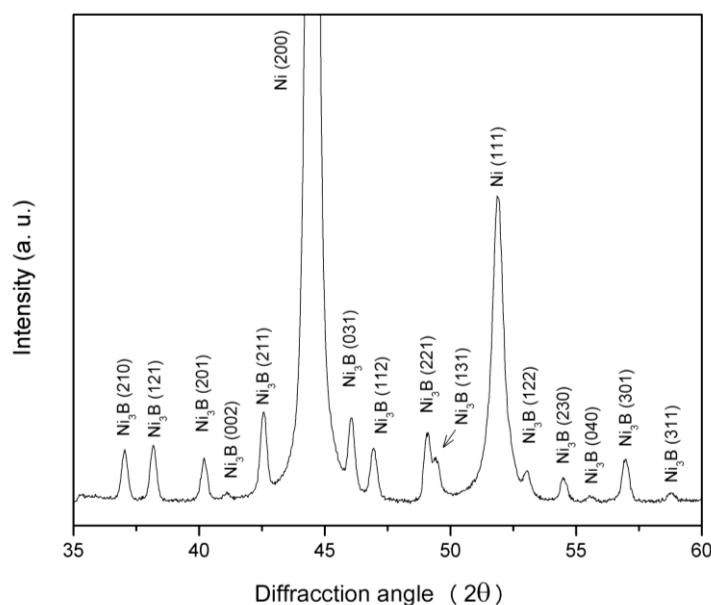


**Figure 6.** XRD spectrum of Ni-B coating (3.4% B) after thermal treatment at 350°C for 1h.

These results reveal that as the treatment of temperature increases, the diffraction signals attributed to metallic Ni are less wider and more intense, indicating that the formation of a crystalline



phase is favored. The XRD spectra verify the formation of the Ni<sub>3</sub>B crystalline phase at 350 ° C for a coating containing 3.4 wt.% B and at 400 ° C for a coating containing 1.8 wt.% of B. These results show that Ni<sub>3</sub>B phase formation is favored with boron content in the coating. Similar behavior was reported by Lee *et al.* [4].

Figure 6 presents the XRD spectra of Ni-B coatings (3.4 wt.% B) after thermal treatment (350°C for 1 h), showing the crystallographic planes of the orthorhombic crystalline (Ni<sub>3</sub>B) phase.

The XRD spectrum of the samples treated at 400 ° C were employed to determine the composition of Ni<sub>3</sub>B in the coatings, to reach this objective, the TOPAS DIFRACC.SUITE 4.2 software was used. Then Ni<sub>3</sub>B composition was used to determine the composition of boron, the results obtained are shown in Table 4. These results indicate that in both cases the concentration of Boron in the coating determined by this method is lower than the boron concentration obtained by ICP. The difference can be explained because this procedure only quantify the boron found as part of the crystal structure as Ni<sub>3</sub>B of a substitutional way in the fcc Ni structure. This indicates that only a fraction of the total boron content in the coating is incorporated in a substitutional, the remaining boron is incorporated interstitially.

**Table 4.** Ni<sub>3</sub>B and Boron composition in the coatings according the TOPAS DIFRACC.SUITE software and it is comparison with the composition obtained by ICP.

Boron composition determined by ICP (wt %)	Rietveld analysis (Software TOPAS 4.2)	
	wt % Ni <sub>3</sub> B	wt % B
1.85	18.5	1.07
3.4	20.3	1.17

In summary, although coatings have different total content of boron (1.85% and 3.4%, measured by ICP), the incorporated amount of substitutional boron is similar (1.07%, 1.17%). As shown above, this may be the reason why both coatings have a crystal size and hardness values very similar (Figure 3).

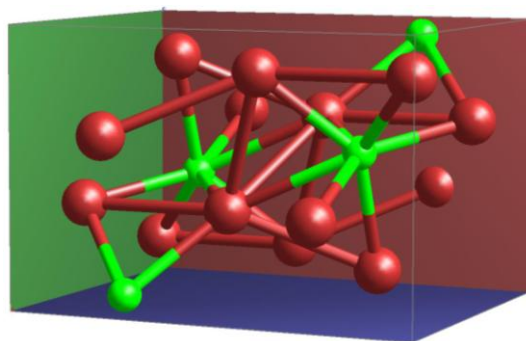


**Figure 7.** 3D graphical representation of the crystallographic plane (100) of the orthorhombic crystal structure (Pnma 62) of Ni<sub>3</sub>B.

### 3.2.2 Hardness

Finally, the effect of thermal treatment on the hardness and crystal size of Ni coatings are shown in Figure 8. Here it can be observed that coating hardness increases significantly as the treatment of temperature increases, reaching its highest value at a temperature of 350 °C for both coatings (independently of B content). At 400 °C, the coating hardness decreases abruptly, and at higher temperatures hardness decreases gradually with increased temperature. This behavior can be attributed to the fact that higher thermal treatment temperatures favor the formation of the Ni<sub>3</sub>B phase and increase the Ni crystal size. Initially (at temperatures below 350 °C) hardness is increased by Ni<sub>3</sub>B phase formation (which has high hardness). At 400 °C the size of the Ni crystals increases considerably and exceeds the size of Ni<sub>3</sub>B phase crystals, diminishing the hardness as reported by Ogihara *et al.* [5].

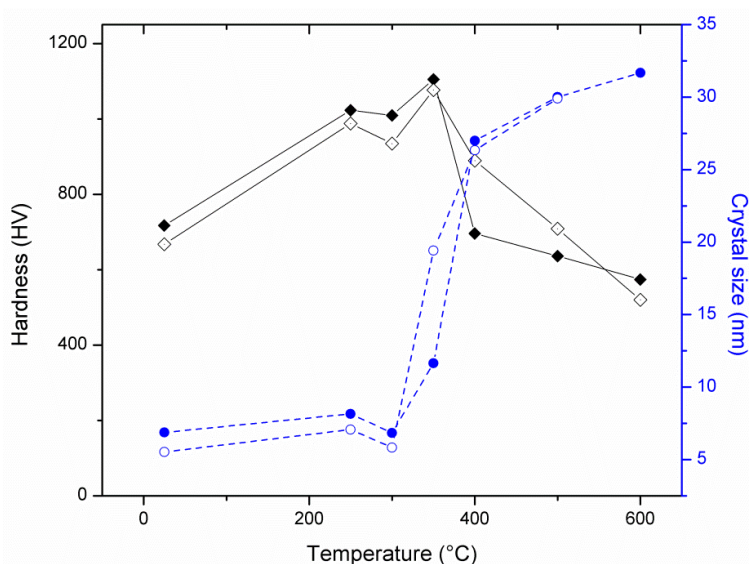


**Figure 8.** Hardness and crystal size variation for Ni-B coatings (with different B composition) after thermal treatment for 1 h: (◆,●) 1.85 % B and (◇, O) 3.4% B.

## 3.3 Evaluation of corrosion resistance

### 3.3.1 Study by polarization curves

The polarization curves obtained for the substrate and Ni-B coatings of different compositions are shown in Figure 9. The results indicate that the curves obtained for electrodeposits Ni-B show a very similar behavior exhibited by the steel substrate (not shown a passive region) differ only in the value of the corrosion potential. The corrosion potential value of these coatings shows a slight decrease with increasing boron content in the coating, similar behavior was observed by Baskaran *et al.* for Ni-B coatings prepared by electroless [9]. The corrosion potential ( $E_{corr}$ ) and corrosion current density ( $j_{corr}$ ) were obtained from these curves using the polarization Tafel extrapolation method; the results are summarized in Table 5.

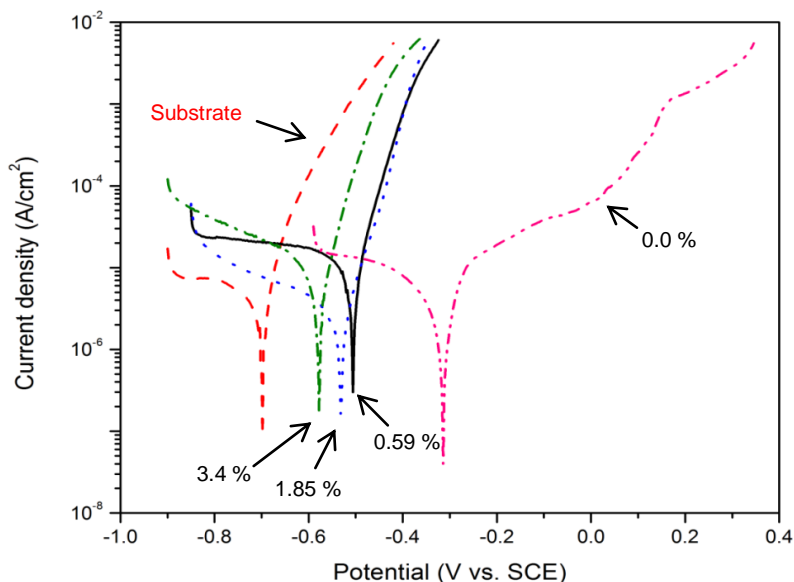


**Figure 9.** Polarization curves obtained in an electrolytic solution consisted of NaCl 5%:(— —) substrate, (— •• —) 0 % B, (—) 0.59 % B, (•••) 1.85 % B and (—•—) 3.4 % B.

**Table 5.** Electrochemical parameters obtained from the polarization curves.

Sample	$E_{corr}$ (V vs SCE)	$j_{corr}$ ( $\mu\text{A}/\text{cm}^2$ )	Tafel slope $b_a$ (mV/dec)
Substrate (steel AISI 1006)	-0.698	11.690	94
Ni (0 % B)	-0.314	8.146	312
Ni-B (0.59 % B)	-0.506	11.037	58
Ni-B (1.85 % B)	-0.532	10.365	66
Ni-B (3.40 % B)	-0.576	11.971	64

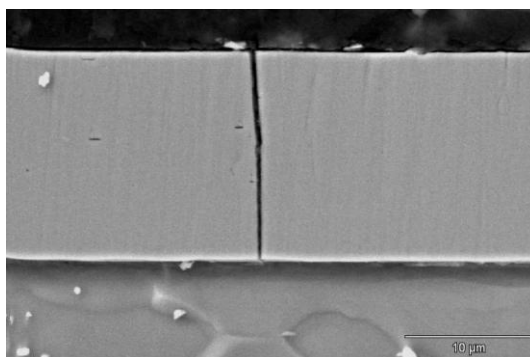


**Figure 10.** SEM image of the transversal cut (3500X) of a Ni-B coating obtained from an electrolytic bath with a concentration of 3 g/L of DMAB.

The corrosion potential for Ni-B coating is the order of -0.51 to -0.58 V vs ESC, these values are very similar to the values reported for Ni-B deposits [9, 28]. While the current density values

(average value:  $11.12 \mu\text{A}/\text{cm}^2$ ) and the Tafel slope values (average value:  $62.7 \text{ mV}/\text{decade}$ ) do not vary significantly with increasing content of B in the coating, this may be due to the dissolution of steel (substrate) occurs during the anodic polarization, which may be possible due to the presence of cracks in the coating. The SEM image of the cross section of these coatings allows verifying that these cracks may reach the substrate affecting its function as a corrosion protective coating (Figure 10).

### 3.3.2 Saline Chamber Test

Figure 11 shows the results obtained for exposition in saline chamber test for Ni coatings with different boron content. Time in which the first red point was observed is defined as the beginning of corrosion of the substrate.

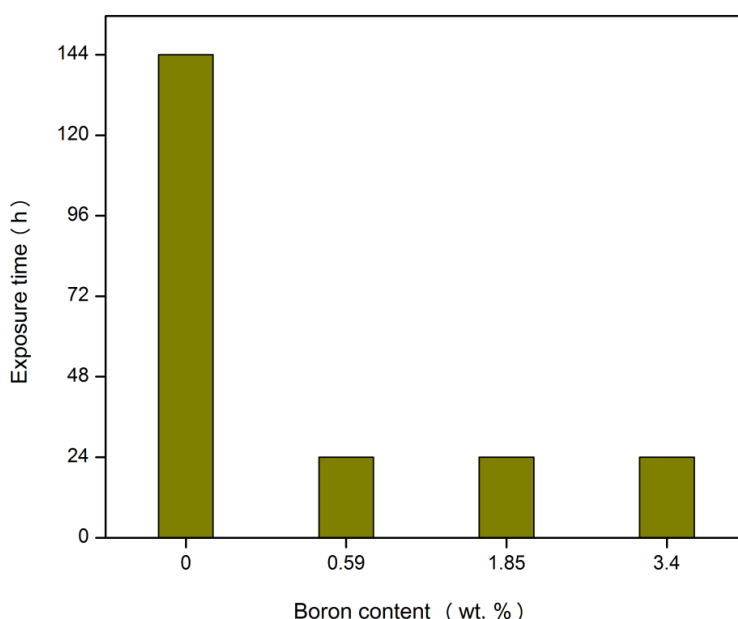


**Figure 11.** Results obtained by salt chamber test, indicating the time when the coating failure (first point of red rust) depending on the composition of boron in the Ni plating.

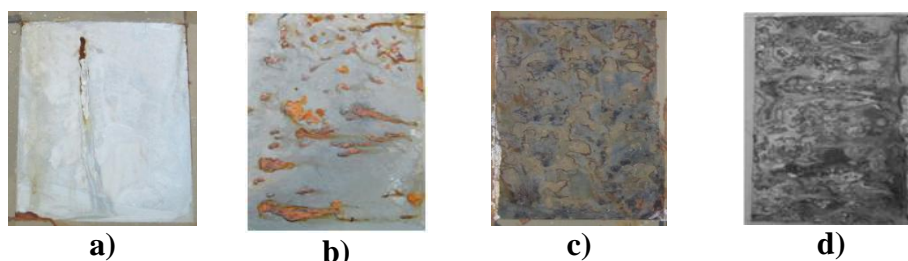


**Figure 12.** Image of the samples after the saline chamber test : a) Ni (0 % B), b) 0.59 %B, c) Ni-B (1.85 % B), d) Ni-B (3.4 % B).

The results indicate that all the Ni-B coatings independently of the boron content, showed products of red corrosion at 24 h of exposure at saline chamber test. This result reveals that the corrosion resistance of the Ni-B coatings are similar and the differences observed in the corrosion potential and exchange current density are not significant to observe changes in the saline chamber test. This can be attributed to corrosion resistance is clearly affected by the presence of cracks which exposes the substrate to the aggressive media (NaCl 5%).

#### 4. CONCLUSIONS

Increased hardness of Ni-B coatings, without thermal treatment, is more influenced by the decrease of crystal size than by the boron composition in the coating. These conditions produce Ni-B coating with high hardness ( $716 \pm 22.5$  HV) at relatively low B concentration (1.85 %).

The effect of thermal treatment on hardness depends on the composition ( $\text{Ni}_3\text{B}$ ) and crystal size. When the coating is treated at a temperature less than  $350\text{ }^\circ\text{C}$ , the increase in hardness is affected primarily by the formation of the  $\text{Ni}_3\text{B}$  crystalline phase. At these temperatures, crystal size is less than 20 nm and does not have a dominant effect. Coatings produced after thermal treatment at temperatures equal to or greater than  $400\text{ }^\circ\text{C}$  showed a decrease of the hardness as a result of the increase in the crystal size. At these temperatures, crystal size is greater than 25 nm and grain size is the dominant factor than the presence of the  $\text{Ni}_3\text{B}$  crystalline phase. This effect may be attributed to the Ni crystal size, which considerably exceeds the size of  $\text{Ni}_3\text{B}$  crystals, minimizing the effect of hardness.

This study confirmed that Ni-B coatings can be produced using a sulfamate electrolyte bath containing DMAB as a boron source. The coatings produced by this process had properties of hardness similar or better than coatings produced from a Watts-type bath.

Unless the obtained Ni-B coatings showed a high hardness, the corrosion resistance is low due to the presence of cracks. To improve the anticorrosion behavior, it is necessary to diminish the presence of cracks. One alternative could be the use of additives in the electrolytic bath, like saccharine [29] or the employ of pulsed current [30]. Another alternative can be to obtain a sublayer of Ni with high corrosion resistance before the Ni-B coating. Studies of the obtaining of multilayer coatings with good corrosion resistance and high hardness are in development.

#### ACKNOWLEDGEMENTS

The authors thank the Mexican Council of Science and Technology (CONACYT) and the Postgraduate Program of Cooperation France-México (PCP) for their financial support of this research and John Dye, a collaborator at CIDETEQ sponsored by the US Peace Corps, for his valuable comments. J. R. Lopez and P.F. Méndez are also grateful to CONACYT for doctoral scholarships.

#### References

1. R. F. Bunshah, *Handbook of Deposition Technologies for Films and Coatings Science, Technology and Applications*, Noyes Publications, New Jersey (1994).
2. G. O. Mallory and J.B. Hajdu, *Electroless Plating: Fundamentals and Applications*, Noyes Publications, New York (1990).

3. Y. W. Riddle and T. O. Bailer, *JOM* Vol. 57, No 4 (2005) 40.
4. K. H. Lee, D. Chang, S.C. Kwon, *Electrochim. Acta*, 50 (2005) 4538.
5. H. Ogihara, K. Udagawa and T. Saji, *Surf. Coat. Tech.*, 206 (2012) 11.
6. K. Krishnaveni, T.S.N. Sankara Narayanan and S.K. Seshadri, *Surf. Coat. Tech.*, 190 (2005) 115.
7. Yu. N. Bekish, S. K. Poznyak, L. S. Tsybulskay and T. V. Gaevskay, *Electrochim. Acta*, 55 (2010) 2223.
8. Q.-L. Rao, G. Bi, Q.-H Lu, H.-W Wang and X.-I Fan, *Appl. Surf. Sci.*, 240 (2005) 28.
9. I. Baskaran, T. S. N. Sankara Narayanan and A. Stephen, *Trans. Inst. Met. Finish.*, 87 (2009) 221.
10. I. Baskaran, R. Sakthi Kumar, T.S.N. Sankara Narayanan and A. Stephen, *Surf. Coat. Tech.*, 200 (2006) 6888.
11. T. Saito, E. Sato, M. Matsuoka and C. Iwapura, *J. Appl. Electrochem.*, 28 (1998) 559.
12. J.-W Yoon, J.-M Koo, J.-W Kim, S.-S Ha, B.-I Noh, C.-Y Lee, J.-H Park, C.-C Shur and S.-Boo Jung, *J. Alloy. Compd.*, 466 (2008) 73.
13. Z. Abdel Hamid, H. B. Hassan and A. M. Attyia, *Surf. Coat. Tech.*, 205 (2010) 2348.
14. C. Domínguez-Ríos, A. Hurtado-Macias, R. Torres-Sánchez, M. A. Ramos and J. González-Hernández, *Ind. Eng. Chem. Res.*, 51 (2012) 7762.
15. R. C. Agarwala and V. Agarwala, *Sadhana-Acad. Proc. Eng. Sci.*, 28 (2003) 475.
16. A. M. Pillai, A. Rajendra and A. K. Sharma, *J. Coat. Technol. Res.*, 9 (2012) 785.
17. P. Peeters, G.v.d. Hoorn, T. Daenen, A. Kurowski and G. Staikov, *Electrochim. Acta*, 47 (2001) 161.
18. K. Krishnaveni, T.S.N. Sankara Narayanan and S.K. Seshadri, *Mater. Chem. Phys.*, 99 (2006) 300.
19. K. Krishnaveni, T. S. N. Sankara Narayanan and S. K. Seshadri, *J. Mater. Sci.*, 44 (2009) 433.
20. S. Arai, S. Kasai and I. Shohji, *J. Electrochem. Soc.*, 157, (2010) D119.
21. D. Baudrand, *Met. Finish.*, 94 (1996) 15.
22. Standard Reference Test Method for Making Potentiostatic and potentiodynamic Anodic Polarization Measurements, Designation: G5-94 (Reapproved 1999), ASTM international, Pennsylvania, United States (1999).
23. Standard Practice for Operating Salt Spray (Fog) Apparatus, Designation B117-09, ASTM international, Pennsylvania, United States (2009).
24. Methods for corrosion testing of metallic and other inorganic coatings on metallic substrates - Rating of test specimens and manufactured articles subjected to corrosion tests, International Organization for Standardization ISO 10289, Genève Switzerland (1999).
25. H. Zhao, L. Liu, J. Zhu, Y. Tang, W. Hu, *Mater. Lett.* 61 (2007) 1605.
26. E. Pompei, L. Magagnin, N. Lecis, P. L. Cavallotti, *Electrochim. Acta*, 54 (2009) 2571.
27. S. W. Banovic, K. Barmak and A. R. Marder, *J. Mater. Sci.*, 33 (1998) 639
28. K. Krishnaveni, T. S. N. Sankara Narayanan, S. K. Seshadri, *J. Alloys Compd.*, 480 (2009) 765.
29. R. Dzedzina, Mária Hagarová, *Int. J. Electrochem. Sci.*, 8 (2013) 8291.
30. S. Ghaziof, W. Gao, *Journal of Alloys and Compounds*, 622 (2015) 918.